PROCEEDINGS OF SCIENCE

Identification and attribution of RFI Sources using NWP departure statistics

Tracy Scanlon,[a,*] **David I. Duncan,**[a] **Alan J. Geer**[a] **and Niels Bormann**[a]

[a] *ECMWF, Shinfield Road, Reading, UK*

E-mail: tracy.scanlon@ecmwf.int, david.duncan@ecmwf.int, alan.geer@ecmwf.int, niels.bormann@ecmwf.int

As numerical weather prediction systems move towards an integrated Earth system approach, the exploitation of lower frequency channels (10 GHz and below) is becoming increasingly important. One of the challenges of using such channels is contamination from Radio Frequency Interference (RFI). This paper demonstrates two methods for the mitigation of such spurious signals focusing on the screening of RFI from geostationary broadcast satellites for the 10.65 GHz channel of AMSR2 and the use of the differences between the background departures from the NWP system to identify RFI in the 6.9 GHz channel of AMSR2.

Radio Frequency Interference Conference (RFI2024)
14-18 October 2024
Bariloche, Argentina

[*] Speaker

 ISSN 1824-8039 . Published by SISSA Medialab.

PoS(RFI2024)026

1. Introduction

ECMWF is increasingly coupling the ocean and atmosphere within its data assimilation and weather forecasting activities. To facilitate this and provide the best available information, channels with sensitivity to the surface will start to be assimilated over open oceans. For microwave imagers, these channels include 6.9 and 10.65 GHz which are both available on the Advanced Microwave Scanning Radiometer 2 (AMSR2). As part of the quality control work for these channels, it was found that both channels are affected by forms of Radio Frequency Interference (RFI). This abstract will describe the methods used to detect and screen out the affected data using departure statistics from the Numerical Weather Prediction (NWP) system of ECMWF.

2. RFI from Geostationary Sources at 10.65 GHz

The background departures (the difference between the observation and the brightness temperature simulated from the background forecast) for the AMSR2 10.65 GHz (v-polarisation, henceforth denoted as v) channel are shown prior to any screening in Figure 1. Strong positive departures (i.e. the observations are much larger than the simulated values) are apparent over Europe in the descending overpass. The descending swaths are the parts of the orbit where the satellite is travelling southwards and AMSR2 is hence viewing towards the equator. Similar patterns in this channel have been previously identified as RFI [1–3]. It is thought that these patterns are a result of the signal from direct broadcast geostationary satellites being reflected off the ocean surface and into the sensor. The 10.69v GHz band is protected with a bandwidth of 100 MHz [4] but is immediately adjacent to a band allocated for space-to-earth transmission [4, 6].

To test this, here we consider the geometry of a direct broadcast satellite with the observation satellite (i.e. AMSR2) as shown in Figure 2 where the x- and y-axes represent North and East respectively and the z-axis is perpendicular to the Earth's surface. From this, we can calculate the glint angle between the directly reflected broadcast signal and the observation beam, as follows:

$$\cos\alpha = \cos\theta_o \cos\theta_s - \sin\theta_o \sin\theta_s \cos\left(\phi_o - \phi_s\right) \tag{1}$$

Where α is the glint angle, θ represents zenith angles and ϕ represents azimuth angles with respect to north and the subscripts o and s denote the observation (sensor) and the broadcast satellites

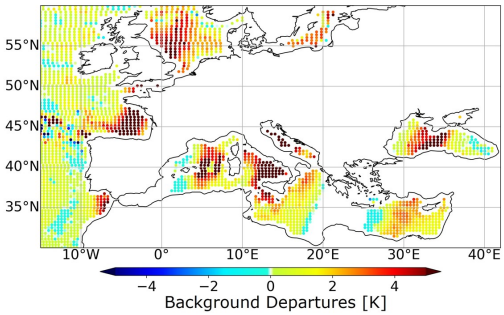

Figure 1: Background departures for the AMSR2 10.65v GHz channel for the 2022-06-02 21h to 9h cycle showing descending overpasses over Europe.

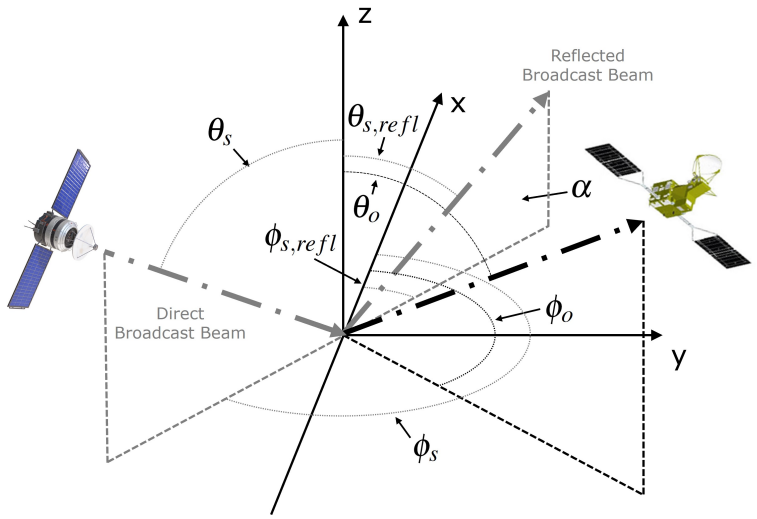

Figure 2: The geostationary satellite / observation satellite geometry and angles used in the calculation of the glint angle.

respectively, as shown in Figure 2. The glint angle is the angle between the observation beam and the reflected solar beam, which is described by $\theta_{s,refl} = \theta_s$ and $\phi_{s,refl} = \phi_s - \pi$ (assuming specular reflection from a horizontal surface).

Using the assumption that the broadcast satellite is in geostationary orbit and is hence positioned over the equator, the only unknown becomes the associated longitude. To identify the likely longitude of the satellites causing the suspected RFI signal, a theoretical study has been performed in which 360 satellites have been placed around the globe at the equator with a 1° longitudinal spacing, at the altitude of a geostationary orbit (42164 km from the centre of the Earth).

The glint angle between these theoretical satellites and AMSR2 is calculated for each observation location (under clear-sky conditions). For all observations where the glint angle is under 3° (chosen to pick out the most central of the glint features), the mean of the background departures is calculated. For those observations where the glint angles are under 10°, the correlation between the glint angle and the background departures are calculated. From the combination of this information, it is possible to determine if the RFI is likely to be caused by a broadcast satellite positioned at a particular longitude. For example, where the mean is high and the correlation is highly negative, it is likely that RFI from direct broadcast satellites is present. In addition, this can be compared to other channels and maps of the background departures and associated observations to confirm the presence of RFI.

Figure 3 shows the results of this method over Europe for a 10-day period in June 2022. it can be seen that there are likely broadcast satellites at three longitudes causing the glint patterns seen over Europe: 30°W, 13°E and 38°E, with the signal at 13°E being the strongest. In each case, the local maximum of the mean background departure and the minimum of the correlation align to within 1°, with small changes being possible due to other effects such as model biases or the impact of the averaging of raw observations onto a 40 km grid in a process known as superobbing.

The glint patterns from each of the identified broadcast satellites correspond to different parts

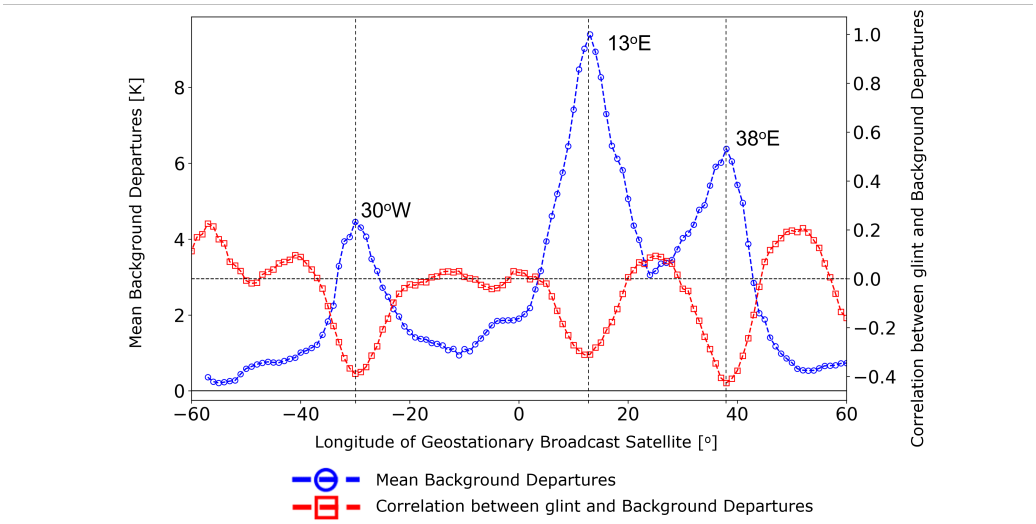

Figure 3: With geostationary satellites placed at 1° longitude spacings (at the equator), the mean of the background departures over Europe is calculated for the locations where the corresponding glint angle is less than or equal to 3° (blue line) and the correlation is that between the background departures and the glint angle for all locations where the glint angle is less than or equal to 10° (red line).

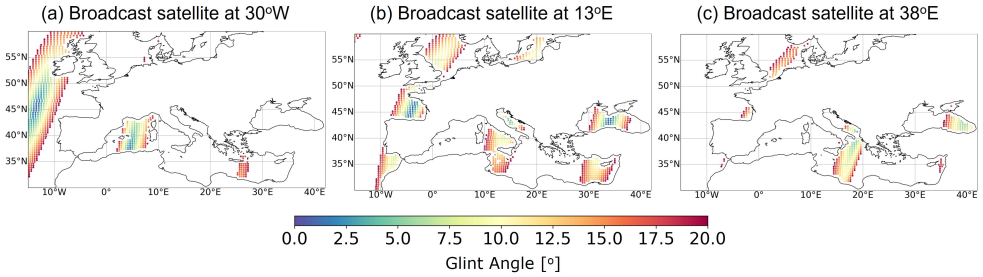

Figure 4: Maps for 2022-07-15T00 for the glint angles of the observations with geostationary satellites placed at (a) 30°W, (b) 13°E and (c) 38°E. The glint angles have a cut off threshold of 20° indicating the area that is screened out by the RFI screening process.

of the high background departures seen over Europe. Figure 4 shows the glint angles for when the broadcast satellite is positioned at the longitudes identified from Figure 3; only those glint angles below 20° are provided to show the areas that are screened out with this threshold. From this Figure, it is clear that the satellite at 13°E causes the largest of the high background departure scar patterns: both that going through the UK and down to Spain and across Italy and through the Black Sea, while the smaller pattern to the East of Spain is caused by the satellite from 30°W. Finally, the satellite at 38°E contributes to the patterns seen to the north of the Netherlands and the south-east of Italy.

3. RFI from Other Sources at 6.9 GHz

To identify RFI sources not related to geostationary broadcast satellites, the difference between adjacent channels has been exploited (as previously used in several studies including [2, 5]). Here,

we consider the 6.9v and 7.3v GHz channels available on AMSR2 due to their spectral proximity. Note that the original intent of the spectral proximity of these channels in the sensor design was to aid in RFI detection and mitigation [6]. Here, instead of using the difference between the observations (as used in previous studies) we calculate the differences between the background departures for these channels, as follows:

$$\Delta_{RFI} := (O_{6.9v} - B_{6.9v}) - (O_{7.3v} - B_{7.3v}) \tag{2}$$

Where Δ_{RFI} is the quantity to be used to detect the potential RFI, O is the observation, B is the simulation of the observation using the model parameters and the subscripts *6.9v* and *7.3v* refer the channels to which these quantities are related. Taking into account the true quantities being observed plus any error terms, this equation can be shown to represent the difference in the RFI present in each channel, as follows:

$$\Delta_{RFI} = RFI_{6.9v} - RFI_{7.3v} + \epsilon \tag{3}$$

Where ϵ represents the errors associated with the observations and the simulations of the observations. This equation results in Δ_{RFI} always being positive when the RFI in the 6.9v GHz channel is larger than that in the 7.3v GHz channel (note we do not implement screening of RFI at 7.3v GHz as the channel is not currently actively assimilated by the NWP system). In reality, the simulations are not perfect and are subject to many different errors (not expanded on here) which will contribute to this value of Δ_{RFI} either negatively or positively. Therefore, to minimise false flagging caused by such errors, we set a threshold for the value of Δ_{RFI} of 2.0 K (found empirically) which allows us to identify the observations most likely affected by RFI.

Figure 5 shows the number of observations in a 2.5 degree grid box which are screened out over the period of a month. Whilst the screening is spread geographically a few areas are more frequently screened. Both the East China sea and the North sea are screened out most frequently and it is thought this may be related to oil platforms in these areas. There is also a linear feature southwest of India where many observations have been screened as RFI which may be related to the Maldives. However, areas where rejections are occasional, such as the line just north of the Equator, and poleward-extending areas in the Pacific and Atlantic, are thought to be false identifications generated by simulation errors in the presence of cloud and precipitation, given these are all areas most frequently affected by precipitation including the inter-tropical convergence zone, the storm tracks and the south Pacific convergence zone.

4. Conclusions

RFI remains a major challenge in an NWP context. With the introduction of surface sensitive channels, we see sources of RFI directly affecting the assimilation of these channels. For AMSR2, we have identified RFI from geostationary direct broadcast satellites at 10.65 GHz and other, potentially ground-based sources at 6.9 GHz. The screening methods presented represent a step forward in the screening of RFI in an NWP context over open oceans however additional work is required to automate the detection of RFI contaminated observations and allow the methods to be applied in a wider context.

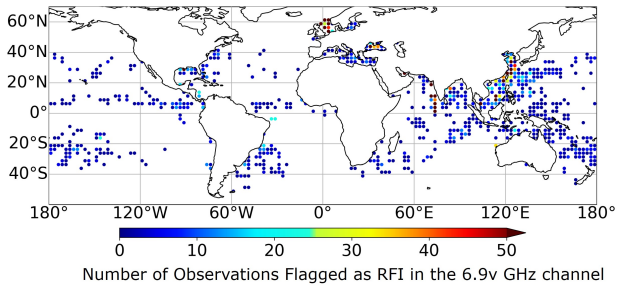

Figure 5: Number of observations screened out using the O-B difference method within a 2.5 degree grid over the course of December 2022.

References

[1] Wu, Y., Li, M., Bao, Y. and Petropoulos, G. P. (2020). "Cross-validation of Radio-Frequency-Interference signature in satellite microwave radiometer observations over the ocean." Remote Sensing, 12, 20, doi:10.3390/rs12203433.

[2] Zabolotskikh, E. V., Mitnik, L. M. and Chapron, B. (2015). "Radio-Frequency Interference identification over oceans for C- and X-band AMSR2 channels." IEEE Geoscience and Remote Sensing Letters, 12, 8, 1705–1709, doi:10.1109/LGRS.2015.2420120.

[3] Draper, D. W. and de Matthaeis, P. (2018). "Radio Frequency Interference trends for the AMSR-E and AMSR2 radiometers." In IGARSS 2018 - 2018 IEEE International Geoscience and Remote Sensing Symposium, pp. 301–304, doi:10.1109/IGARSS.2018.8518061.

[4] NTIA (2016). "National telecommunications and information administration: United states department of commerce." United States Frequency Allocation Chart, [Accessed 11-01-2024].

[5] Draper, D. and Newell, D. (2015). "An assessment of Radio Frequency Interference using the GPM microwave imager." In 2015 IEEE International Geoscience and Remote Sensing Symposium (IGARSS), pp. 5170–5173, doi:10.1109/IGARSS.2015.7326998.

[6] Kazumori, M., Geer, A. J. and English, S. J. (2016). "Effects of all-sky assimilation of GCOM-W/AMSR2 radiances in the ECMWF Numerical Weather Prediction system." Quarterly Journal of the Royal Meteorological Society, 142(695), 721–737, doi:https://doi.org/10.1002/qj.2669.